Received 26 June; accepted 23 September 1997.

1. Nobes, C. D. & Hall, A. Rho, rac, and cdc GTPases regulate the assembly of multimolecular focal complexes associated with actin stress fibers, lamellipodia, and filopodia. *Cell* **81,** 53–62 (1995).
2. Kozma, R., Ahmed, S., Best, A. & Lim, L. The GTPase-activating protein n-chimaerin cooperates with Rac1 and Cdc42Hs to induce the formation of lamellipodia and filopodia. *Mol. Cell. Biol.* **15,** 1942–1952 (1995).
3. Manser, E., Leung, T., Salihuddin, H., Zhao, Z. S. & Lim, L. A brain serine/threonine protein kinase activated by Cdc42 and Rac1. *Nature* **367,** 40–46 (1994).
4. Manser, E., Leung, T., Salihuddin, H., Zhao, Z. S. & Lim, L. A non-receptor tyrosine kinase that inhibits the GTPase activity of $p21^{cdc42}$. *Nature* **363,** 364–367 (1993).
5. Symons, M. *et al.* Wiskott–Aldrich syndrome protein, a novel effector for the GTPase CDC42Hs, is implicated in actin polymerization. *Cell* **84,** 723–734 (1996).
6. Miki, H., Miura, K. & Takenawa, T. N-WASP, a novel actin-depolymerizing protein, regulates the cortical cytoskeletal rearrangement in a PIP2-dependent manner downstream of tyrosine kinases. *EMBO J.* **15,** 5326–5335 (1996).
7. Burbelo, P. D., Drechsel, D. & Hall, A. A conserved binding motif defines numerous candidate target proteins for both Cdc42 and Rac GTPases. *J. Biol. Chem.* **270,** 29071–29074 (1995).
8. Aspenstrom, P., Lindberg, U. & Hall, A. Two GTPases, Cdc42 and Rac, bind directly to a protein implicated in the immunodeficiency disorder Wiskott–Aldrich syndrome. *Curr. Biol.* **15,** 5725–5731 (1996).
9. Lamarche, N. *et al.* Rac and Cdc42 induce actin polymerization and G1 cell cycle progression independently of p65PAK and the JNK/SAPK MAP kinase cascade. *Cell* **87,** 519–529 (1996).
10. Nishida, E., Maekawa, S. & Sakai, H. Cofilin, a protein in porcine brain that binds to actin filaments and inhibits their interactions with myosin and tropomyosin. *Biochemistry* **23,** 5307–5317 (1984).
11. Aizawa, H. *et al.* Identification, characterization, and intracellular distribution of cofilin in *Dictyostelium discoideum*. *J. Biol. Chem.* **270,** 10923–10932 (1995).
12. Pantaloni, D. & Carlier, M.-F. How profilin promotes actin filament assembly in the presence of thymosin β4. *Cell* **75,** 1007–1014 (1993).
13. Fukuoka, M., Miki, H. & Takenawa, T. Identification of N-WASP homologs in human and rat brain. *Gene* **196,** 43–48 (1997).
14. Komuro, R., Sasaki, T., Takaishi, K., Orita, S. & Takai, Y. Involvement of Rho and Rac small G proteins and Rho GDI in Ca^{2+}-dependent exocytosis from PC12 cells. *Genes to Cells* **1,** 943–951 (1996).
15. Self, A. J. & Hall, A. Purification of recombinant Rho/Rac/G25K from *Escherichia coli*. *Meth. Enzymol.* **256,** 3–10 (1995).

Acknowledgements. We thank S. Suetsugu and Y. Banzai for their skilful technical assistance. This work was supported in part by a Grant-in-Aid for Cancer Research from the Ministry of Education, Science, and Culture of Japan and a Grant-in-Aid for Research for the Future Program from the Japan Society for the Promotion of Science.

Correspondence and requests for materials should be addressed to T.T. (e-mail: takenawa@hgc.ims.u-tokyo.ac.jp).

Cleavage of CAD inhibitor in CAD activation and DNA degradation during apoptosis

Hideki Sakahira*, Masato Enari* & Shigekazu Nagata*†

** Department of Genetics, Osaka University Medical School, 2-2 Yamada-oka, Suita, Osaka 565, Japan*

† Osaka Bioscience Institute, 6-2-4 Furuedai, Suita, Osaka 565, Japan

Various molecules such as cytokines and anticancer drugs, as well as factor deprivation, rapidly induce apoptosis (programmed cell death)[1,2], which is morphologically characterized by cell shrinkage and the blebbing of plasma membranes and by nuclear condensation[3,4]. Caspases, particularly caspase 3, are proteases that are activated during apoptosis and which cleave substrates such as poly(ADP-ribose) polymerase, actin, fodrin, and lamin[5,6]. Apoptosis is also accompanied by the internucleosomal degradation of chromosomal DNA[7–9]. In the accompanying Article[10], we have identified and molecularly cloned a caspase-activated deoxyribonuclease (CAD) and its inhibitor (ICAD). Here we show that caspase 3 cleaves ICAD and inactivates its CAD-inhibitory effect. We identified two caspase-3 cleavage sites in ICAD by site-directed mutagenesis. When human Jurkat cells were transformed with ICAD-expressing plasmid, occupation of the receptor Fas, which normally triggers apoptosis, did not result in DNA degradation. The ICAD transformants were also resistant to staurosporine-induced DNA degradation, although staurosporine still killed the cells by activating caspase. Our results indicate that activation of CAD downstream of the caspase cascade is responsible for internucleosomal DNA degradation during apoptosis, and that ICAD works as an inhibitor of this process.

We have shown that the growing cells carry an inactive form of CAD and its inhibitor ICAD in the cytosol. Mouse ICAD purified from mouse WR19L cells is a protein of relative molecular mass (M_r) 32K, which can inhibit CAD-induced DNA degradation in nuclei as well as its DNase activity on plasmid DNA. In contrast to growing cells, lysates from Fas-activated apoptotic cells do not have ICAD activity (data not shown), suggesting that ICAD could be inactivated by an apoptotic signal. A candidate in activator is caspase 3, which is itself activated during apoptosis[1,11–13]. To test whether ICAD is cleaved by caspase 3, we incubated ICAD purified from mouse WR19L cells with caspase 3. As shown in Fig. 1a, caspase-3-treated ICAD could no longer inhibit CAD-induced DNA degradation in nuclei or its DNase activity on plasmid DNA; also, the 32K ICAD protein was specifically cleaved by caspase 3 (Fig. 1b).

Molecular cloning of ICAD complementary DNAs has indicated that ICAD exists in two forms, ICAD-L for the long form and ICAD-S for the short form[10], which seem to be generated by alternative splicing. Both ICAD-L and ICAD-S carry two putative

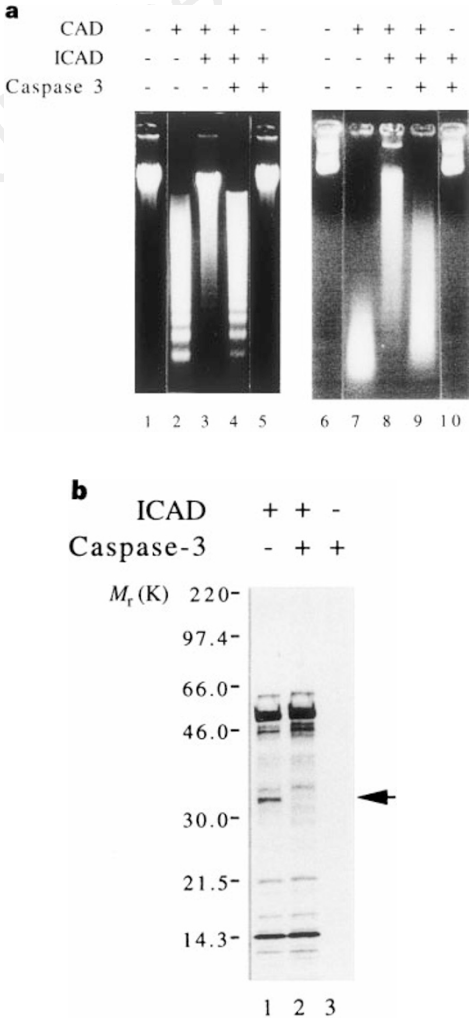

Figure 1 Inactivation of ICAD by caspase-3 cleavage. **a**, Native purified ICAD[10] (100 ng) was incubated with 15 ng caspase 3 in buffer A (see Methods). Lysates from Fas-activated W4 cells (20 μg) (lanes 1–5) or caspase-3-activated, partially purified CAD (5 ng) (lanes 6–10) were mixed with 25 ng caspase-3-treated or untreated ICAD. CAD activity was assayed with mouse nuclei (lanes 1–5) or with plasmid DNA (lanes 6–10) using CAD (lanes 2 and 7), CAD and ICAD (lanes 3 and 8), CAD and caspase-3-treated ICAD (lanes 4 and 9), or caspase-3-treated ICAD alone (lanes 5 and 10). **b**, Purified ICAD (100 ng) was treated with 15 ng caspase 3, electrophoresed on a 10–20% gradient polyacrylamide gel and visualized by silver staining. Lanes: 1, ICAD before caspase 3 treatment; 2, ICAD after caspase 3 treatment; 3, 15 ng caspase 3. ICAD is indicated by an arrow.

cleavage sites for caspase 3 (Fig. 2a); specifically, DEPD and DAVD at amino-acid positions 117 and 224 conform well to the consensus cleavage sites for caspase (refs 3, 14, 15). Caspase requires aspartic acid at the P1 position of the cleavage site[14,15]. To test whether caspase 3 cleaves ICAD at these positions (Fig. 2a), the aspartic acid residues at the cleavage sites were singly or doubly mutated to glutamic acid. Recombinant glutathione-*S*-transferase (GST) fusion protein for each ICAD mutant was produced in *Escherichia coli* and purified to homogeneity. Treatment of wild-type ICAD-L (L/WT) with caspase 3 yielded two bands of M_r 40K and 12K (Fig. 2b). The upper band is a fusion protein consisting of GST and the amino-terminal portion of ICAD, whereas the lower band is actually two bands derived from the middle and carboxy-terminal portions of ICAD. When Asp 117 was mutated (L/D117E), the upper band generated by caspase 3 shifted to an M_r of 52K, whereas mutation of Asp 224 (L/D224E) shifted the lower band to an M_r of 26K. Furthermore, the double mutation at both sites (L/dm) generated an ICAD that was resistant to caspase 3. Similar results were obtained with mutants of ICAD-S. We then assayed for inhibition by mutated ICAD of CAD-induced DNA degradation. Like native ICAD, caspase 3 treatment of recombinant ICAD destroyed its inhibitory activity (Fig. 2c). ICADs carrying a single mutation at Asp 117 or double mutations at Asp 117 and 224 were still functional after treatment with caspase 3. On the other hand, ICAD, particularly ICAD-S, carrying the intact cleavage site at Asp 117 was sensitive to caspase 3. These results indicate that the cleavage of ICAD at Asp 117 by caspase 3 inactivates ICAD, and that mutation at Asp 117 can generate caspase-3-resistant ICAD.

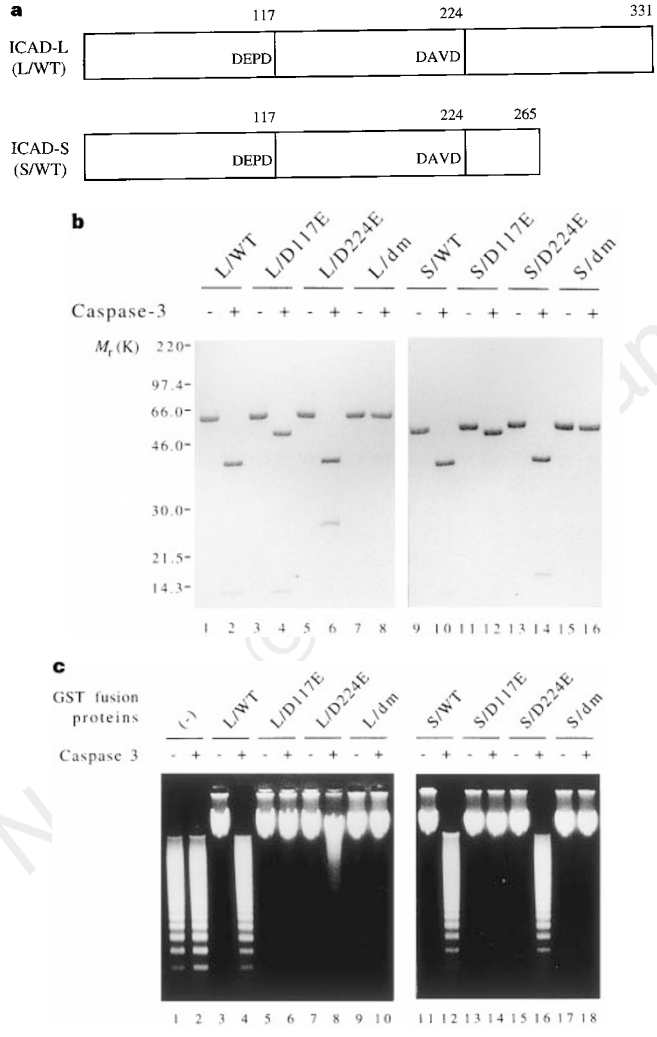

Figure 2 Identification of caspase 3 cleavage sites in ICAD. Recombinant GST fusion proteins with ICAD-L and ICAD-S, and their mutants, were produced in *E. coli* and purified as described in Methods. **a**, Putative caspase 3 cleavage sites in ICAD-L and ICAD-S. **b**, Recombinant GST fusion proteins (2 μg) with ICAD-L (lanes 1–8) or ICAD-S (lanes 9–16) were incubated with 75 ng caspase 3. Samples were run on a 10–20% gradient polyacrylamide gel before (lanes 1, 3, 5, 7, 9, 11, 13 and 15) and after (lanes 2, 4, 6, 8, 10, 12, 14 and 16) caspase 3 treatment, and stained with Coomassie brilliant blue. The GST–ICAD proteins were: wild-type (L/WT and S/WT), singly mutated at D117 (L/D117E and S/D117E) or at D224 (L/D224E and S/D224E), or doubly mutated at D117 and D224 (L/dm and S/dm). **c**, 10 ng GST–ICAD-L (lanes 3–10) or GST–ICAD-S (lanes 11–18) were incubated with (lanes 2, 4, 6, 8, 10, 12, 14, 16 and 18) or without (lanes 1, 3, 5, 7, 9, 11, 13, 15 and 17) 15 ng caspase 3 as described in Methods. Cell lysate from Fas-activated W4 cells (20 μg) was then added and CAD activity assayed on liver nuclei.

Human Jurkat cells can be killed by agonistic anti-Fas antibody or by a high concentration of staurosporine, and in both cases cell death is accompanied by internucleosomal cleavage of chromosomal DNA[16] (A. Kawahara and S.N., unpublished results). To investigate the effect of ICAD on DNA degradation during apoptosis, wild-type ICAD-L and ICAD-S, as well as their caspase-3-resistant double mutants, were tagged with the Flag epitope and their expression plasmids introduced into Jurkat cells. The stable transformant clones expressing ICAD were selected by western blotting using anti-Flag antibody (Fig. 3a). The expression of Fas in all transformant clones was the same as in parental cells (data not shown). When parental Jurkat cells were treated with anti-Fas antibody, their chromosomal DNA was degraded into 180-base-pair (bp) multimers within 4 h (Fig. 3b). On the other hand, transformants expressing wild-type ICAD-L or ICAD-S, or their caspase-3-resistant mutants, did not show any DNA fragmentation, even after a 6-h incubation with anti-Fas antibody. Similarly, when Jurkat cells were incubated with 10 μM staurosporine, their chromosomal DNA was degraded within 2 h; however, this degradation was completely inhibited by overexpression of wild-type ICAD-L or ICAD-S. These results indicate that ICAD specifically blocks the DNase(s) that is activated during apoptosis.

The killing of cells by staurosporine was then followed by flow cytometry using annexin V[17]. As shown in Fig. 3c, most of the parental Jurkat cells, as well as the transformants expressing wild-type ICAD-L or ICAD-S, became annexin-V-positive (indicative of cell death) within 2 h of treatment with staurosporine. When cell death was assayed by the MTT method, which determines the integrity of mitochondria[18], the results also indicated that the cells (parental Jurkat and ICAD transformants) treated with staurosporine died within 2 h (data not shown). This killing was accompanied by the cleavage of 116K poly(ADP-ribose) polymerase to an 85K protein (Fig. 3d). Furthermore, when caspase 3 activity in the cytosol was determined by using a fluorescent substrate, the activity in ICAD transformant cells after staurosporine treatment was comparable to that in parental Jurkat cells (Fig. 3e). The anti-Fas antibody also killed the Jurkat and ICAD transformants by activating caspase 3, although the killing process was slow compared with that induced by staurosporine (data not shown). These results indicate that the cell can die without DNA degradation, probably as a result of cleavage of various important cellular substrates by caspases.

We have shown that ICAD can be inactivated by caspase 3 and that overexpression of ICAD in human Jurkat cells blocks DNA degradation during apoptosis. Mouse ICAD-L shares significant sequence similarity with one of the subunits of human DFF (DFF45, for DNA-fragmentation factor 45)[19] and seems to be the murine counterpart of DFF45. Purified human DFF consists of 45K and 40K subunits and causes DNA fragmentation in nuclei when treated with caspase 3. This is also a property of the inactive CAD that we have identified[10]. DFF itself does not have DNase activity, suggesting that DFF is not human CAD. It has been proposed that when DFF45 is cleaved by caspase 3, DFF enters the nucleus and activates a

nuclear DNase[19]. In contrast, mouse CAD has an intrinsic DNase activity, which ICAD inhibits by binding to it. These results may indicate that ICAD can bind not only CAD, but also another molecule (DFF40) that regulates a DNase. The DNase regulated by DFF may be CAD or a CAD-like DNase because overexpression of ICAD inhibits DNA degradation in the apoptotic process in human cells.

Caspase 3 inactivates ICAD by cleaving it. We originally thought that CAD could be inhibited in cells only by caspase-resistant ICAD: however, overexpression of wild-type ICAD in Jurkat cells completely blocks DNA degradation induced by Fas engagement, as well as by staurosporine. These results suggest that an ICAD-inhibitable DNase is activated during apoptosis and that this activation can be triggered by different stimuli. As ICAD inhibits CAD, but does not inhibit DNase I or II (ref. 10), we conclude that CAD or a CAD-like DNase is responsible for the DNA degradation that occurs in apoptosis, at least in human Jurkat cells where apoptosis is induced by Fas or staurosporine. Most ICAD introduced into the cells is quickly degraded by these apoptotic stimuli (H.S. and S.N., unpublished results), indicating that a small amount of ICAD is sufficient to inhibit CAD activity, or that the concentration of CAD is minimal. Apoptosis can be induced in thymocytes by glucocorticoids[9] and in various cells by factor or serum deprivation[2]. To assess the generality of CAD's involvement in apoptosis, it will be necessary to study the effect of ICAD in other systems.

Studies on programmed cell death in *C. elegans* have indicated that DNase activity is not essential for cell killing[20]. One mouse cell line was killed by the action of cytotoxic lymphocytes without apparent DNA fragmentation[21]. Here the transformants expressing ICAD were killed by staurosporine treatment without cleavage of chromosomal DNA. Caspase was fully active under these conditions, which places the apoptotic DNase downstream of the caspases and indicates that cleavage of cellular substrates such as actin, Rho–GDI and fodrin is sufficient to kill the cells[5,6]. In addition to cleavage of DNA, apoptotic stimuli induce the condensation and fragmentation of nuclei[3]. It is not yet clear whether it is DNA degradation or cleavage of nuclear proteins such as poly(ADP-ribose) polymerase and lamin that is responsible for the morphological changes in cells[4,22,23]: cells that carry a fully activated caspase and do not suffer DNA degradation will clarify this point. Finally, it has been proposed that degradation of chromosomal DNA is involved in the cleaning up of dead cells, by facilitating phagocytosis or by preventing transformation of the phagocytosing cells by intact DNA from the dying cells[22]. The genes encoding CAD and ICAD will be useful for addressing these questions. □

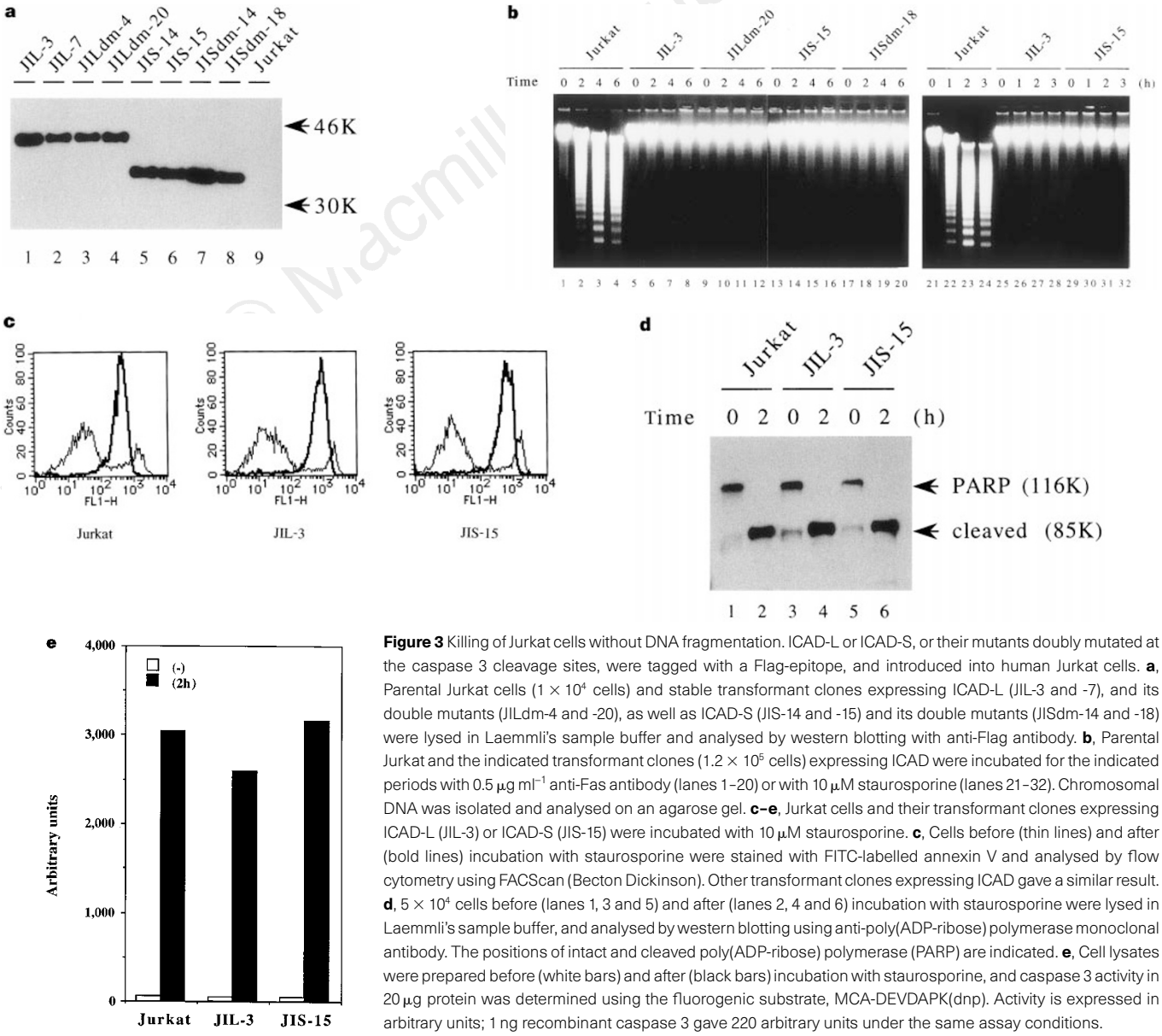

Figure 3 Killing of Jurkat cells without DNA fragmentation. ICAD-L or ICAD-S, or their mutants doubly mutated at the caspase 3 cleavage sites, were tagged with a Flag-epitope, and introduced into human Jurkat cells. **a**, Parental Jurkat cells (1×10^4 cells) and stable transformant clones expressing ICAD-L (JIL-3 and -7), and its double mutants (JILdm-4 and -20), as well as ICAD-S (JIS-14 and -15) and its double mutants (JISdm-14 and -18) were lysed in Laemmli's sample buffer and analysed by western blotting with anti-Flag antibody. **b**, Parental Jurkat and the indicated transformant clones (1.2×10^5 cells) expressing ICAD were incubated for the indicated periods with 0.5 μg ml^{-1} anti-Fas antibody (lanes 1–20) or with 10 μM staurosporine (lanes 21–32). Chromosomal DNA was isolated and analysed on an agarose gel. **c–e**, Jurkat cells and their transformant clones expressing ICAD-L (JIL-3) or ICAD-S (JIS-15) were incubated with 10 μM staurosporine. **c**, Cells before (thin lines) and after (bold lines) incubation with staurosporine were stained with FITC-labelled annexin V and analysed by flow cytometry using FACScan (Becton Dickinson). Other transformant clones expressing ICAD gave a similar result. **d**, 5×10^4 cells before (lanes 1, 3 and 5) and after (lanes 2, 4 and 6) incubation with staurosporine were lysed in Laemmli's sample buffer, and analysed by western blotting using anti-poly(ADP-ribose) polymerase monoclonal antibody. The positions of intact and cleaved poly(ADP-ribose) polymerase (PARP) are indicated. **e**, Cell lysates were prepared before (white bars) and after (black bars) incubation with staurosporine, and caspase 3 activity in 20 μg protein was determined using the fluorogenic substrate, MCA-DEVDAPK(dnp). Activity is expressed in arbitrary units; 1 ng recombinant caspase 3 gave 220 arbitrary units under the same assay conditions.

Methods

Purified ICAD, and assay for CAD and ICAD. Purification of ICAD from mouse WR19L cells has been described[10]. The final preparation (active fractions from the Superdex-200 gel-filtration column) was heated at 90 °C for 15 min and centrifuged at 100,000*g* for 30 min; the supernatant was used as purified ICAD. CAD activity was determined by *in vitro* assay for apoptosis using mouse liver nuclei, or by measuring DNase activity using plasmid DNA as substrate[10]. ICAD activity was assayed by inhibition of CAD activity. The cytosolic fraction from Fas-activated cells was used as a source of activated CAD[10]. In some cases, partially purified CAD (100 ng) (resource-S fraction[10]) was incubated with 150 ng caspase 3 at 4 °C for 12 h and at 30 °C for 1 h in 100 μl buffer A (10 mM HEPES-KOH, pH 7.0, 5 mM $MgCl_2$, 5 mM EGTA, 10% glycerol, 1 mM DTT) containing 50 mM NaCl and 100 μg ml^{-1} BSA, and used as activated CAD after inactivating caspase 3 with Ac-DEVD-cho.

Expression of ICAD in *E. coli*. To generate the D117E and D224E mutants, ICAD-S and I-CAD-L cDNAs were mutated by recombinant PCR[24] using 20-nucleotide primers carrying the mutated nucleotides. The D117E/D224E double mutants were generated by replacing the N-terminal half of the D224E mutant with that of D117E mutant, using the *Bgl*/II site between D117 and D224. The wild-type and mutant cDNAs were fused to the GST gene of pGEX-2T[128/129]. pGEX-2T[128/129] is derived from pGEX-2T (Pharmacia) by in-frame insertion of the Flag-epitope tag and a heart-muscle kinase-recognition sequence following the GST gene[25]. The fusion proteins were expressed in *E. coli* AD202, and purified by glutathione–Sepharose-4B (Pharmacia) according to the manufacturer's instructions. Recombinant ICAD eluted from the glutathione column was purified on a Mono-Q HR5/5 column with a NaCl gradient in buffer A containing 0.02% Tween-20.

Transformation of Jurkat cells, cell-death assay and western blotting. Wild-type ICAD-S and ICAD-L and their double mutants were tagged with the Flag epitope at their N termini and ligated into the pEF-BOS vector[26]. Human Jurkat cells were co-transfected with ICAD expression plasmids and pBLIIhyg by electroporation[27]. Hygromycin B(800 μg ml^{-1})-resistant transformants were picked and expanded. Expression of ICAD in individual clones was analysed by western blotting with anti-Flag monoclonal antibody (clone M2, Kodak). To bring about apoptosis, Jurkat and ICAD-transformant cells (2.5×10^5 cells per ml) were incubated at 37 °C with 0.5 μg ml^{-1} of mouse anti-human Fas monoclonal antibody (clone CH11, MBL) or 10 μM staurosporine. Cell death was assayed by using the annexin V method[17] (R & D System kit). DNA fragmentation was assayed as described[27]. Proteolysis of poly(ADP-ribose) polymerase was determined by western blotting using a mouse monoclonal antibody against human poly(ADP-ribose) polymerase (clone C-2-10)[28]. To determine cytosolic caspase 3 activity, a peptide (DEVDAPK) carrying the caspase-3-recognition sequence was coupled to the highly fluorescent (7-methoxycoumarin-4-yl) acetyl group (MCA) and its quenching 2,4-dinitrophenyl (Dnp) group, and the product MCA-DEVDAPK(dnp) used as a substrate as described[11].

Received 20 November; accepted 1 December 1997.

1. Nagata, S. Apoptosis by death factor. *Cell* **88,** 355–365 (1997).
2. Raff, M. C. Social controls on cell survival and cell death. *Nature* **356,** 397–400 (1992).
3. Wyllie, A. H., Kerr, J. F. R. & Currie, A. R. Cell death: the significance of apoptosis. *Int. Rev. Cytol.* **68,** 251–306 (1980).
4. Earnshaw, W. C. Nuclear changes in apoptosis. *Curr. Opin. Cell Biol.* **7,** 337–343 (1995).
5. Henkart, P. A. ICE family protease: mediators of all apoptotic cell death? *Immunity* **4,** 195–201 (1996).
6. Martin, S. & Green, D. Protease activation during apoptosis: death by a thousand cuts. *Cell* **82,** 349–352 (1995).
7. Compton, M. M. A biochemical hallmark of apoptosis: internucleosomal degradation of the genome. *Cancer Metast. Rev.* **11,** 105–119 (1992).
8. Wyllie, A. H., Morris, R. G., Smith, A. L. & Dunlop, D. Chromatin cleavage in apoptosis: association with condensed chromatin morphology and dependence on macromolecular synthesis. *J. Pathol.* **142,** 66–77 (1984).
9. Wyllie, A. H. Glucocorticoid-induced thymocyte apoptosis is associated with endogenous endonuclease activation. *Nature* **284,** 555–556 (1980).
10. Enari, M. *et al.* A caspase-activated DNase that degrades DNA during apoptosis, and its inhibitor ICAD. *Nature* **391,** 43–50 (1998).
11. Enari, M., Talanian, R. V., Wong, W. W. & Nagata, S. Sequential activation of ICE-like and CPP32-like proteases during Fas-mediated apoptosis. *Nature* **380,** 723–726 (1996).
12. Longthorne, V. & Williams, G. Caspase activity is required for commitment to Fas-mediated apoptosis. *EMBO J.* **16,** 3805–3812 (1997).
13. Armstrong, R. C. *et al.* Fas-induced activation of the cell death-related protease CPP32 is inhibited by Bcl-2 and by ICE family protease inhibitors. *J. Biol. Chem.* **271,** 16850–16855 (1996).
14. Thornberry, N. A. *et al.* A combinatorial approach defines specificities of members of the caspase family and granzyme B. *J. Biol. Chem.* **272,** 17907–17911 (1997).
15. Talanian, R. V. *et al.* Substrate specificities of caspase family proteases. *J. Biol. Chem.* **272,** 9677–9682 (1997).
16. Chinnaiyan, A. M. *et al.* Molecular ordering of the cell death pathway. *J. Biol. Chem.* **271,** 4573–4576 (1996).
17. Koopman, G. *et al.* Annexin V for flow cytometric detection of phosphatidylserine expression on B cells undergoing apoptosis. *Blood* **84,** 1415–1420 (1994).
18. Mosmann, T. Rapid colorimetric assay for cellular growth and survival: application to proliferation and cytotoxicity assays. *J. Immunol. Method.* **65,** 55–63 (1983).
19. Liu, X., Zou, H., Slaughter, C. & Wang, X. DFF, a heterodimeric protein that functions downstream of caspase-3 to trigger DNA fragmentation during apoptosis. *Cell* **89,** 175–184 (1997).
20. Ellis, R. E., Yuan, J. & Horvitz, H. R. Mechanisms and functions of cell death. *Annu. Rev. Cell Biol.* **7,** 663–698 (1991).
21. Ucker, D. S. *et al.* Genome digestion is a dispensable consequence of physiological cell death mediated by cytotoxic T lymphocytes. *Mol. Cell. Biol.* **12,** 3060–3069 (1992).
22. Peitsch, M., Mannherz, H. & Tschopp, J. The apoptosis endonucleases: cleaning up after cell death? *Trends Cell Biol.* **4,** 37–41 (1994).
23. Cohen, J. J., Duke, R. C., Fadok, V. A. & Sellins, K. S. Apoptosis and programmed cell death in immunity. *Annu. Rev. Immunol.* **10,** 267–293 (1992).
24. Higuchi, R. in *PCR Protocols: A guide to Methods and Applications* 177–188 (Academic, San Diego, 1990).
25. Blanar, M. A. & Rutter, W. J. Interaction cloning: identification of a helix-loop-helix zipper protein that interacts with c-Fos. *Science* **256,** 1014–1018 (1992).
26. Mizushima, S. & Nagata, S. pEF-BOS: a powerful mammalian expression vector. *Nucleic Acids Res.* **18,** 5322 (1990).
27. Itoh, N. *et al.* The polypeptide encoded by the cDNA for human cell surface antigen Fas can mediate apoptosis. *Cell* **66,** 233–243 (1991).
28. Lamarre, D. *et al.* Structural and functional analysis of poly(ADP-ribose) polymerase: an immunological study. *Biochim. Biophys. Acta* **950,** 147–160 (1988).

Acknowledgements. We thank R. V. Talanian for the caspase 3 expression plasmid, G. G. Poirier for anti-human poly(ADP-ribose) polymerase, M. A. Blanar for pGEX-2T[128/129], and S. Kumagai for secretarial assistance. This work was supported in parts by Grants-in-Aid from the Ministry of Education, Science, Sports and Culture in Japan.

Correspondence and requests for materials should be addressed to S.N. (e-mail: nagata@genetic.med.osaka-u.ac.jp).

Poly(A)- and poly(U)-specific RNA 3′ tail shortening by *E. coli* ribonuclease E

Hongjin Huang*, Jian Liao† & Stanley, N. Cohen*†

*Departments of * Genetics and † Medicine, Stanford University School of Medicine, Stanford, California 94305-5120, USA*

Ribonuclease (RNase) E is an extensively studied enzyme from *Escherichia coli* whose site-specific endoribonuclease activity on single-stranded RNA has a central role in the processing of ribosomal RNA, the degradation of messenger RNA and the control of replication of ColE1-type plasmids (for recent reviews, see refs 1–3). Here we report a previously undetected activity of RNase E: the ability to shorten 3′ poly(A)- and poly(U)-homopolymer tails on RNA molecules. This activity, which leaves a 6-nucleotide adenylate or a 1-nucleotide uridylate remnant on primary transcripts, resides in the amino-terminal region of RNase E and does not require other protein cofactors. Addition of a 3′-terminal phosphate group prevents both removal of the poly(A) tail and endonucleolytic cleavage within primary transcripts, but has no effect on the cleavage of transcripts with tails that have already been truncated. The ability of RNase E to shorten poly(A) tails, together with the effect of tail length on endonucleolytic cleavage within primary transcripts, suggests a mechanism by which RNase E may exercise overall control over RNA decay.

During our investigation of RNase E cleavage of 3′ polyadenylated RNAI, the antisense repressor of replication of ColE1-type plasmids[4,5], we observed that poly(A) tails were dramatically shortened under assay conditions in which polynucleotide phosphorylase (PNPase) and RNase II—the two *E. coli* enzymes that have 3′-to-5′ exonucleolytic activity[1,2,6–9]—were not expected to function. To investigate this observation, histidine-tagged full-length RNase E and its N-terminal endoribonucleolytic domain (N-Rne) were overexpressed in *E. coli* and affinity-purified. The N-Rne polypeptide, which contains the first 498 amino acids of the 1,061-amino-acid protein[10] but lacks the PNPase binding site at the C-terminal end of RNase E[11], was further purified to homogeneity by elution from preparative SDS–polyacrylamide gels, followed by renaturation

CORRIGENDUM

doi:10.1038/nature15532

Corrigendum: Cleavage of CAD inhibitor in CAD activation and DNA degradation during apoptosis

Hideki Sakahira, Masato Enari & Shigekazu Nagata

Nature **391,** 96–99 (1998); doi:10.1038/34214

Recently, it has come to our attention that in Fig. 1a of this Letter, lanes 1 and 5 appear to be duplicated and lanes 6 and 10 appear to be duplicated. It is unclear how this happened. We have repeated the experiment (see Fig. 1 of this Corrigendum) and the results were as described in the original Letter. The Supplementary Information to this Corrigendum contains the source data used to generate the corrected Fig. 1. Our conclusions are unaffected.

Supplementary Information is available in the online version of this Corrigendum.

Correspondence should be addressed to S.N. (snagata@ifrec.osaka-u.ac.jp).

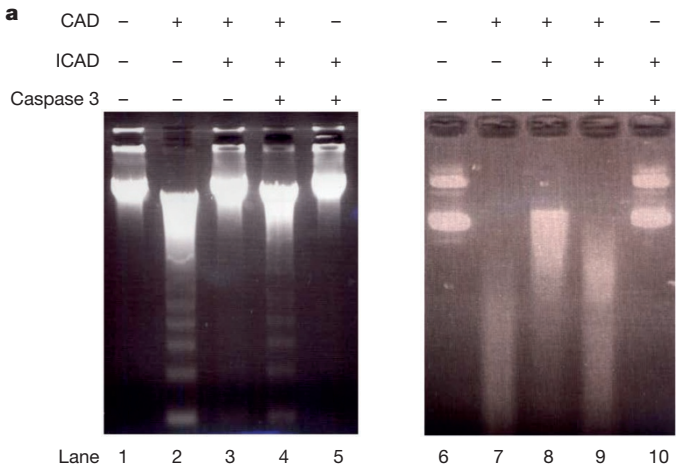

Figure 1 | This is the corrected Fig. 1a of the original Letter.